

Cold gas and young stars in tidally-disturbed ellipticals at $z=0$

P. Serra^{*} and T. A. Oosterloo

ASTRON, Postbus 2, 7990 AA Dwingeloo, the Netherlands

Accepted 2009 October 13. Received 2009 October 13; in original form 2009 October 02

ABSTRACT

We present an analysis of the neutral hydrogen and stellar populations of elliptical galaxies in the Tal et al. (2009) sample. Our aim is to test their conclusion that the continuing assembly of these galaxies at $z \sim 0$ is essentially gas-free and not accompanied by significant star formation. In order to do so, we make use of H I data and line-strength indices available in the literature. We look for direct and indirect evidence of the presence of cold gas during the recent assembly of these objects and analyse its relation to galaxy morphological fine structure.

We find that $\geq 25\%$ of ellipticals contain H I at the level of $M(\text{H I}) > 10^8 M_{\odot}$, and that $M(\text{H I})$ is of the order of a few percent of the total stellar mass. Available data are insufficient to establish whether galaxies with a disturbed stellar morphology are more likely to contain H I. However, H I interferometry reveals very disturbed gas morphology/kinematics in all but one of the detected systems, confirming the continuing assembly of many ellipticals but also showing that this is not necessarily gas-free. We also find that all very disturbed ellipticals have a single-stellar-population-equivalent age < 4 Gyr. We interpret this as evidence that $\sim 0.5\text{--}5\%$ of their stellar mass is contained in a young population formed during the past ~ 1 Gyr. Overall, a large fraction of ellipticals seem to have continued their assembly over the past few Gyr in the presence of a mass of cold gas of the order of 10% of the galaxy stellar mass. This material is now observable as neutral hydrogen and young stars.

Key words: galaxies: evolution – galaxies: ISM – galaxies: stellar content.

1 INTRODUCTION

The role of dissipationless galaxy merging in the assembly of early-type galaxies is currently under debate. On the one hand, it appears to be necessary to produce the boxy, slowly-rotating galaxies which populate the high-mass end of the red sequence (e.g., Faber et al. 1997; Kormendy et al. 2009, and references therein). On the other hand, dissipative processes are required to explain a number of structural, kinematical and stellar-population properties of intermediate- and low-mass early-type galaxies (e.g., Bender et al. 1992; Emsellem et al. 2007; Hopkins et al. 2009, and references therein). Furthermore, the tight scaling relations observed in the local Universe place a rather conservative upper limit on the fraction of stellar mass assembled via dissipationless merging (e.g., Nipoti et al. 2003, 2009). Finally, cold gas is actually observed in a large fraction of early-type galaxies in the nearby Universe (e.g., Morganti et al. 2006; Combes et al. 2007).

Based on deep imaging of a volume-limited sample of nearby elliptical galaxies with $M_B \leq -20$, and following earlier work by, e.g., Malin & Carter (1983) and Schweizer & Seitzer (1992), Tal et al. (2009, hereafter T09) find signatures of recent dynamically-violent assembly in a remarkably large fraction of objects, $\sim 75\%$. Analysing galaxies' $B - V$ colour, they argue that ellipticals outside

cluster environments continue to grow at $z=0$ mostly through gas-free accretions. If correct, this conclusion would have implications for a number of properties of local ellipticals. This follows from a large number of numerical studies showing that the presence of even a modest amount of gas ($\sim 10\text{--}20\%$ of the baryonic mass) in a binary merger can change the stellar mass-distribution and orbits in the early-type remnant relative to the gas-free case (e.g., Jesseit et al. 2005, 2007; Hopkins et al. 2009). Observable quantities such as ellipticity, isophote disciness/boxiness, anisotropy and light profile are affected by the gas content of the progenitor galaxies.

Although most of these numerical simulations focus on binary major or minor mergers, early-type galaxies in a Λ CDM Universe form following a sequence of many interactions with widely varying mass ratio and degree of dissipation. In other words, galaxies are much more likely to grow via continuous assembly of smaller units of varying gas content rather than a few major events, in a way strongly dependent on their environment (e.g., De Lucia et al. 2006; Naab et al. 2007; Parry et al. 2009). Within this framework, as in the binary merger case, a galaxy formed following a gas-free path (e.g., one residing in the centre of a massive cluster, where little cold gas can penetrate) should be significantly different from one that experienced dissipation (e.g., Bournaud et al. 2007). It is therefore interesting to estimate the mass of cold gas present during the continuing assembly of ellipticals over the last few Gyr and test T09 conclusion that this is indeed negligible.

The approach taken in this Letter is to look for neutral hydro-

^{*} E-mail: serra@astron.nl

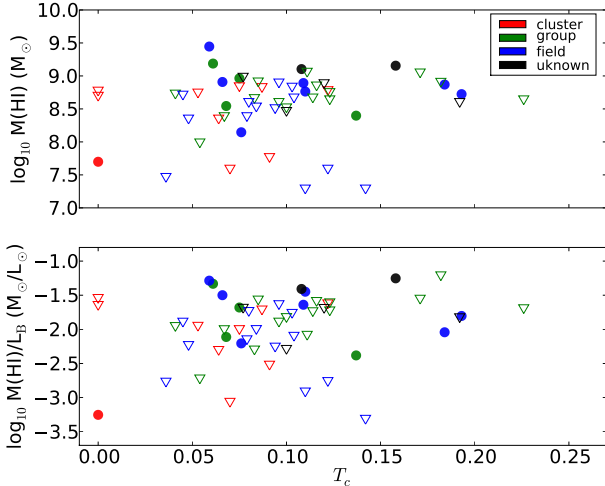


Figure 1. H I content of galaxies in the T09 sample. Circles are H I-detected galaxies, triangles are upper limits on the H I mass. Colour represents the environment as reported by T09.

gen and young stellar populations in galaxies in the T09 sample. Both properties could be regarded as marginally important with respect to the broad cosmological picture of galaxy evolution. After all, work over the past decades shows that young stars and cold gas amount to just a few percent of the total galaxy stellar mass of $z=0$ ellipticals. However, as explained above, even modest amounts of gas can have important effects on fundamental properties of these objects. We would like to clarify what kind of data analysis is necessary in order to detect this gas. Work along this line has been carried out by a number of authors during the past few years. We summarise it together with our results in the discussion section.

2 NEUTRAL HYDROGEN

All galaxies in the T09 sample have been observed in the 21-cm line by the HIPASS survey (Meyer et al. 2004). The noise in the HIPASS spectra is ~ 15 mJy in ~ 13 -km/s-wide channels. It corresponds to a 3σ flux of ~ 2.4 Jy-km/s over 200 km/s, which we take as the typical width of the H I profile. Therefore, the HIPASS $M(\text{H I})$ detection limit varies in the range 0.1 - $1.2 \times 10^9 M_\odot$ as a function of distance for the T09 sample¹. This is not very deep and indeed, after inspection of the HIPASS spectra, we find that only 2 galaxies are detected: IC 1459 and IC 4889. We searched the literature for deeper H I observations. This resulted in 12 more detections and 9 upper limits deeper than those provided by HIPASS (derived with the same criterion described above). In one more galaxy, NGC 6868, H I is detected in absorption against the central radio continuum source (Oosterloo, priv. comm.) and estimating its $M(\text{H I})$ is not possible with current data. We refer to Table 1 for details on the H I data.

In Fig.1 we plot $M(\text{H I})$ and $M(\text{H I})/L_B$ against the tidal parameter T_c introduced by T09. T_c is designed as a way of quantifying the amount of morphological fine structure and is larger for galaxies with higher disturbance. In the figure, colour represents galaxy environment following the T09 division of the sample in

cluster, group, field and unknown environment. Overall, we find H I in/around $\sim 1/4$ of ellipticals, and mostly outside the cluster environment. Because of the inhomogeneity of the data, we conclude that $\geq 25\%$ of ellipticals contain H I at the 10^8 - M_\odot level. $M(\text{H I})$ can be as high as a few times $10^9 M_\odot$, corresponding to at most a few percent of the total stellar mass. Given the many upper limits, we cannot establish whether highly-disturbed ellipticals host more H I in/around their stellar body than more relaxed objects.

Most of the H I data used here are taken with single-dish telescopes. These have a beam of several arcmin *FWHM* and we have discarded 4 detections that are likely caused by the presence of a late-type neighbour within the same beam. However, a number of observations taken with interferometers are available and allow us to study the actual spatial distribution of the H I around about half of the detected galaxies. Here we comment on individual galaxies for which radio interferometry is available.

IC 1459 shows a number of H I filaments surrounding the stellar body; the galaxy resides in a rich group with many gas-rich disc galaxies. IC 4889 hosts a strongly-warped disc/ring, but the poor spatial resolution of the ATCA data may hide a more complicated configuration. NGC 2865 is a known recent-merger remnant with H I associated to a number of stellar shells. NGC 2974 hosts a regular H I ring aligned with the stellar body. NGC 4472, the brightest galaxy in the Virgo cluster, shows an H I cloud that suggests on-going interaction with a dwarf neighbour. NGC 5018 shows a filament of gas stretching across its stellar body and connecting two neighbours. NGC 5077 is likely in the process of acquiring gas from a late-type companion as a broad tail of H I connects the two systems and H I clouds are scattered around them. NGC 5903 hosts kinematically-disturbed H I distributed along the galaxy minor axis and two gas tails connected to the edge of this distribution.

Overall, interferometric data show a disturbed H I configuration, signature of on-ongoing or recent (~ 1 Gyr) gas accretion, in all but one of the detected ellipticals. Considering gas consumption in star formation and tidal-tail gas lost to the inter-galactic medium, it is plausible that many ellipticals have continued their assembly until recently in the presence of a mass of cold gas as high as $\sim 10\%$ of their total stellar mass. Given the many high upper limits on $M(\text{H I})$, deeper H I observations would be required to establish the actual fraction of ellipticals that host neutral hydrogen at this level in the T09 sample. However, we can state that this is $\geq 25\%$, in agreement with deep observations where H I is found in about half of the targets (Morganti et al. 2006). It is clear that the presence of significant amounts of cold gas during the recent assembly of these systems is fairly common outside cluster environments.

3 STELLAR POPULATIONS

Fully corrected line-strength indices measured from optical spectra and brought onto the Lick/IDS system are available in the literature for 38/55 galaxies in the T09 sample. For 34 of them indices within an $R_e/10$ aperture are given by Thomas et al. (2005) or Annibali et al. (2006). Indices for a few additional objects and measured over slightly different apertures are available in Sánchez-Blázquez et al. (2007) and Serra et al. (2008). We refer to Table 1 for details on the line-strength data.

In Fig.2 we plot $H\beta$, an age-sensitive index, against $[\text{MgFe}]$, a metallicity indicator nearly insensitive to $[\alpha/\text{Fe}]$ variations². Galax-

¹ $M(\text{H I}) = 2.36 \times 10^5 F(\text{H I}) / (\text{Jy} \cdot \text{km/s}) (d/\text{Mpc})^2 M_\odot$

² $[\text{MgFe}] = \sqrt{\text{Mgb} \times (\text{Fe5270} + \text{Fe5335})/2}$

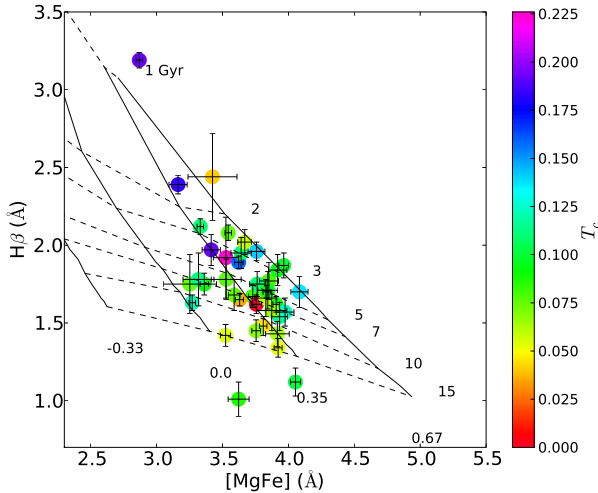


Figure 2. $H\beta$ vs. $[MgFe]$ for the 38 galaxies in the T09 sample with available line-strength indices. Colour codes the tidal parameter T_c defined in T09. The model grid represents SSP models from Thomas et al. (2003). Solid lines are models of fixed metallicity with $[Z/H]$ labelled at the bottom of the grid. Dashed lines are models of fixed stellar age with.

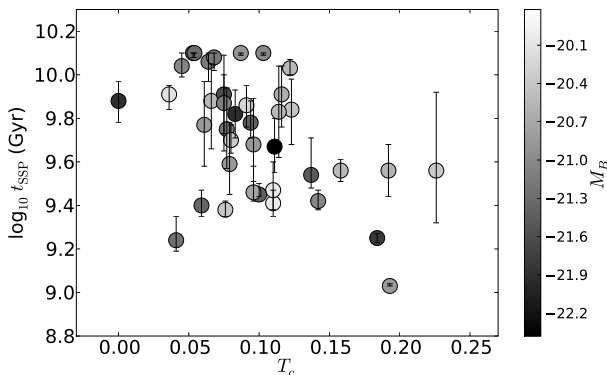


Figure 3. t_{SSP} vs. T_c for the 38 galaxies in the T09 sample with available line-strength indices. The grey-scale codes M_B .

ies are plotted on top of a model grid which represents solar- $[\alpha/Fe]$ single-stellar-population (SSP) models of Thomas et al. (2003). Colour represents T_c . The figure shows that *high- T_c ellipticals tend to be younger than more relaxed objects*. In particular, there are no old galaxies with $T_c > 0.13$. The galaxy with very large central $H\beta$ is NGC 2865, a known gas-rich merger remnant.

We derive best-fitting SSP-equivalent age and metallicity (t_{SSP} and $[Z/H]_{SSP}$) by comparing line-strength indices to predictions from Thomas et al. (2003) models. The comparison is performed on the $[MgFe]$ - $H\beta$ plane shown in Fig.2. We have verified that t_{SSP} , the most relevant parameter for our study, is in agreement with values taken from Thomas et al. (2005), Annibali et al. (2007), Sánchez-Blázquez et al. (2007) and Serra et al. (2008) despite the fact that we neglect the effect of $[\alpha/Fe]$. We list t_{SSP} values in Table 1.

In Fig.3 we plot t_{SSP} against T_c , with grey-scale representing M_B . While we do not see a clean correlation between t_{SSP} and T_c , highly-disturbed ellipticals clearly stand out as they are all fairly young ($t_{SSP} < 4$ Gyr). On the contrary, most galaxies with low T_c

are older, although there are a number of weakly-disturbed objects with young ages too. We note that high- T_c galaxies are not younger because of being systematically fainter than more relaxed objects.

If a galaxy hosts stars with a spread in age, t_{SSP} is strongly biased towards the age of the youngest stars (see Serra & Trager 2007 for a thorough discussion of this effect). Therefore, it is likely that galaxies with a t_{SSP} of just a few Gyr host recently-formed stars on top of an old, dominant population. We estimate the young-to-total stellar mass fraction M_y/M_t by comparing $H\beta$ and $[MgFe]$ to predictions from solar- $[\alpha/Fe]$, two-SSP models built based on Thomas et al. (2003) SSPs. Since the number of free parameters is large, we assume that the old population has an age of 13 Gyr and that the young population has solar metallicity. We let the metallicity of the old population (which dominates $[MgFe]$) - see Serra & Trager 2007) and M_y/M_t free to vary, and fix the age of the young population t_y to 300 Myr and 1 Gyr in two different fitting iterations. Given the known degeneracy between t_y and M_y/M_t this approach allows us to more easily estimate the allowed range for M_y/M_t .

We find that ellipticals with $t_{SSP} < 4$ Gyr contain 0.5-5% of their stellar mass in stars formed 300 Myr to ~ 1 Gyr ago. Given the many approximations involved in this analysis these numbers should be taken with some care. Nevertheless, it is hard to question that many ellipticals, and in particular all highly-disturbed objects, are consistent with having formed up to a few percent of their stellar mass within the past ~ 1 Gyr. We note that it would have been impossible to reach this conclusion based on optical photometry only. Indeed, the best-fitting two-SSP models predict $B - V$ colours in the range 0.9-1.1 with typical 1σ uncertainty below 0.1 dex. The only exception is NGC 2865, which is predicted to have $B - V \sim 0.8$.

4 DISCUSSION AND CONCLUSIONS

Neutral hydrogen observations and line-strength index analysis of the stellar populations of ellipticals in the T09 sample reveal that a large fraction of these galaxies continued their assembly during the past few Gyr in the presence of a mass of cold gas of *at least* a few percent of the total galaxy stellar mass. This gas is now detected in the form of H I and through young stellar sub-populations.

H I interferometry reveals that in nearly all cases the detected gas is morphologically/kinematically disturbed and mostly found in tails/filaments, sometimes clearly associated to the optical morphological disturbances. This, and the presence of young stars, confirm T09 conclusion that the assembly of elliptical galaxies continues to $z=0$. However, it does not agree with their conclusion that this assembly is essentially gas-free. In fact, H I observations could be regarded as yet one more tool to reveal the on-going assembly of these systems, complementary to deep optical imaging (see Morganti et al. 2006; Oosterloo et al. 2007; Grossi et al. 2009).

Our estimate of the mass of cold gas recently accreted by ellipticals is in qualitative agreement with the mass accretion rate derived by T09 themselves. They estimate that nearby ellipticals are still growing at $z=0$ at a rate of 20%-in-mass per Gyr. Evidence of this on-going assembly is particularly strong in the field and in galaxy groups, where most small galaxies around a given elliptical are gas rich. It is therefore reasonable to expect that such a conspicuous mass assembly is accompanied by an accretion of cold gas of *at least* a few percent of the total galaxy stellar mass.

Despite this high incidence of disturbed H I systems, elliptical galaxies with very regular gas distributions do exist (e.g., NGC 2974; more examples can be found in Morganti et al. 2006; Oosterloo et al. 2007). These systems could be evolved versions of

the galaxies that show disturbed H I at $z=0$, i.e., galaxies for which gas accretion was important many Gyr ago and whose recent history has been quiet enough for this gas to settle.

Another interesting point is that while we find that optically disturbed ellipticals are systematically younger than relaxed objects, and interpret this as evidence of their continuing, gas-rich assembly, not all ellipticals with H I are young (e.g., NGC 5846; other cases are known outside the T09 sample, e.g., NGC 4278 in Morganti et al. 2006). Clearly, the dynamics of the accretion plays a very important role in determining the effect of gas on structure and (distribution of) stellar population of the accreting galaxy. Understanding where the young stars and cold gas are, and what their kinematics is, is as important as estimating their mass.

Our results agree with previous work on this subject. Sanchez-Blazquez et al. (2009) analyse the stellar population of high- z early-type galaxies selected by van Dokkum (2005) to be “dry”-merger remnants. They find that highly disturbed objects are on average younger than relaxed ones, and that their line-strength indices are consistent with the presence of a few-percent-in-mass of young stars. This is in agreement with early results from Schweizer et al. (1990) who find the H β index to be systematically higher for ellipticals with morphological fine structure at any given absolute magnitude. Finally, Donovan et al. (2007) look at the H I properties of a sample of local galaxies selected in the same way as the van Dokkum (2005) objects. They find that many of these systems host a significant mass of H I whose disturbed morphology and kinematics make them consistent with having recently accreted cold gas.

Following the conclusions of a large number of numerical studies, the direct or indirect detection of gas present during the assembly of elliptical galaxies may have important implications for many structural properties of these objects. We have shown that using only observables such as colours measured over large apertures one risks to neglect the evidence of this gas because of the lower sensitivity to the presence of a modest, but nevertheless significant, mass of cold gas or young-stars.

REFERENCES

- Annibali F., Bressan A., Rampazzo R., Zeilinger W. W., 2006, *A&A*, 445, 79
- Annibali F., Bressan A., Rampazzo R., Zeilinger W. W., Danese L., 2007, *A&A*, 463, 455
- Appleton P. N., Pedlar A., Wilkinson A., 1990, *ApJ*, 357, 426
- Bender R., Burstein D., Faber S. M., 1992, *ApJ*, 399, 462
- Bottinelli L., Gouguenheim L., 1977, *A&A*, 60, L23
- Bottinelli L., Gouguenheim L., 1979a, *A&A*, 74, 172
- Bottinelli L., Gouguenheim L., 1979b, *A&A*, 76, 176
- Bournaud F., Jog C. J., Combes F., 2007, *A&A*, 476, 1179
- Combes F., Young L. M., Bureau M., 2007, *MNRAS*, 377, 1795
- De Lucia G., Springel V., White S. D. M., Croton D., Kauffmann G., 2006, *MNRAS*, 366, 499
- Donovan J. L., Hibbard J. E., van Gorkom J. H., 2007, *AJ*, 134, 1118
- Emsellem E., Cappellari M., Krajnović D., van de Ven G., Bacon R., Bureau M., Davies R. L., de Zeeuw P. T., Falcón-Barroso J., Kuntschner H., McDermid R., Peletier R. F., Sarzi M., 2007, *MNRAS*, 379, 401
- Faber S. M., Tremaine S., Ajhar E. A., Byun Y.-I., Dressler A., Gebhardt K., Grillmair C., Kormendy J., Lauer T. R., Richstone D., 1997, *AJ*, 114, 1771
- Grossi M., di Serego Alighieri S., Giovanardi C., Gavazzi G., Giovanelli R., Haynes M. P., Kent B. R., Pellegrini S., Stierwalt S., Trinchieri G., 2009, *A&A*, 498, 407
- Haynes M. P., Herter T., Barton A. S., Benensohn J. S., 1990, *AJ*, 99, 1740
- Hopkins P. F., Cox T. J., Dutta S. N., Hernquist L., Kormendy J., Lauer T. R., 2009, *ApJS*, 181, 135
- Huchtmeier W. K., 1994, *A&A*, 286, 389
- Jesseit R., Naab T., Burkert A., 2005, *MNRAS*, 360, 1185
- Jesseit R., Naab T., Peletier R. F., Burkert A., 2007, *MNRAS*, 376, 997
- Kim D.-W., Jura M., Guhathakurta P., Knapp G. R., van Gorkom J. H., 1988, *ApJ*, 330, 684
- Knapp G. R., Faber S. M., Gallagher J. S., 1978, *AJ*, 83, 11
- Knapp G. R., Turner E. L., Cunniffe P. E., 1985, *AJ*, 90, 454
- Kormendy J., Fisher D. B., Cornell M. E., Bender R., 2009, *ApJS*, 182, 216
- Lake G., Schommer R. A., 1984, *ApJ*, 280, 107
- Lewis B. M., 1987, *ApJS*, 63, 515
- Malin D. F., Carter D., 1983, *ApJ*, 274, 534
- McNamara B. R., Sancisi R., Henning P. A., Junor W., 1994, *AJ*, 108, 844
- Meyer M. J., Zwaan M. A., Webster R. L., Staveley-Smith L., Ryan-Weber E., Drinkwater M. J., Barnes D. G., Howlett M., Kilborn V. A., Stevens J., Waugh M., Pierce M. J., Bhathal R., de Blok W. J. G., Disney M. J., Ekers R. D., Freeman K. C., et al. 2004, *MNRAS*, 350, 1195
- Morganti R., de Zeeuw P. T., Oosterloo T. A., McDermid R. M., Krajnović D., Cappellari M., Kenn F., Weijmans A., Sarzi M., 2006, *MNRAS*, 371, 157
- Naab T., Johansson P. H., Ostriker J. P., Efstathiou G., 2007, *ApJ*, 658, 710
- Nipoti C., Londrillo P., Ciotti L., 2003, *MNRAS*, 342, 501
- Nipoti C., Treu T., Bolton A. S., 2009, *ArXiv e-prints*
- Oosterloo T. A., Morganti R., Sadler E. M., van der Hulst T., Serra P., 2007, *A&A*, 465, 787
- Parry O. H., Eke V. R., Frenk C. S., 2009, *MNRAS*, 396, 1972
- Sánchez-Blázquez P., Forbes D. A., Strader J., Brodie J., Proctor R., 2007, *MNRAS*, 377, 759
- Sanchez-Blazquez P., Gibson B. K., Kawata D., Cardiel N., Balcells M., 2009, *ArXiv e-prints*
- Sansom A. E., Hibbard J. E., Schweizer F., 2000, *AJ*, 120, 1946
- Schimminovich D., van Gorkom J. H., van der Hulst J. M., Malin D. F., 1995, *ApJL*, 444, L77
- Schweizer F., Seitzer P., 1992, *AJ*, 104, 1039
- Schweizer F., Seitzer P., Faber S. M., Burstein D., Dalle Ore C. M., Gonzalez J. J., 1990, *ApJL*, 364, L33
- Serra P., Trager S. C., 2007, *MNRAS*, 374, 769
- Serra P., Trager S. C., Oosterloo T. A., Morganti R., 2008, *A&A*, 483, 57
- Tal T., van Dokkum P. G., Nelan J., Bezanson R., 2009, *ArXiv e-prints*
- Thomas D., Maraston C., Bender R., 2003, *MNRAS*, 339, 897
- Thomas D., Maraston C., Bender R., Mendes de Oliveira C., 2005, *ApJ*, 621, 673
- Tonry J. L., Dressler A., Blakeslee J. P., Ajhar E. A., Fletcher A. B., Luppino G. A., Metzger M. R., Moore C. B., 2001, *ApJ*, 546, 681
- van Dokkum P. G., 2005, *AJ*, 130, 2647
- Weijmans A.-M., Krajnović D., van de Ven G., Oosterloo T. A., Morganti R., de Zeeuw P. T., 2008, *MNRAS*, 383, 1343

Table 1. Sample properties.

galaxy	d (Mpc)	M_B	$B - V$	T_c	$M(\text{H I})$ ($10^8 M_\odot$)	$\text{H}\beta$ (\AA)	Mgb (\AA)	$\langle\text{Fe}\rangle$ (\AA)	t_{SSP} (Gyr)	env	references
	(1)	(2)	(3)	(4)	(5)	(6)	(7)	(8)	(9)	(10)	
IC 1459	29.2	-21.47	0.96	0.137	2.5	1.70±0.10	5.38±0.10	3.10±0.08	3.5 ^{+1.7} _{-0.4}	G	a,d,v
IC 3370	26.8	-20.59	0.89	0.192	<4.1	1.97±0.10	4.27±0.10	2.73±0.09	3.6 ^{+1.2} _{-0.9}	U	a,e,v
IC 4797	28.1	-20.36	0.92	0.226	<4.5	1.92±0.26	4.52±0.18	2.75±0.10	3.6 ^{+4.7} _{-1.5}	G	a,e,x
IC 4889	29.2	-20.54	0.88	0.158	14.3	1.89±0.04	4.18±0.04	3.14±0.05	3.6 ^{+0.4} _{-0.4}	U	a,f,y
NGC 0584	20.1	-20.40	0.92	0.076	1.4	2.08±0.05	4.33±0.04	2.90±0.03	2.4 ^{+0.2} _{-0.2}	F	a,g,x
NGC 0596	21.8	-20.03	0.90	0.110	<0.2	2.12±0.05	3.95±0.04	2.81±0.03	2.6 ^{+0.4} _{-0.3}	F	a,h,x
NGC 0720	24.1	-20.86	0.96	0.079	<2.5	1.77±0.12	5.17±0.11	2.87±0.09	3.9 ^{+0.3} _{-1.1}	F	a,i,x
NGC 1199	33.1	-20.49	0.97	0.067	<2.5	-	-	-	-	G	a,j
NGC 1209	35.8	-20.62	0.95	0.116	<7.3	1.54±0.09	4.88±0.09	3.17±0.08	8.1 ^{+2.8} _{-2.4}	G	a,e,v
NGC 1395	24.1	-21.43	0.94	0.094	<3.3	1.62±0.05	5.21±0.04	2.93±0.03	6.0 ^{+1.6} _{-0.9}	F	a,e,x
NGC 1399	20.0	-21.16	0.98	0.064	<2.3	1.43±0.08	5.20±0.16	2.95±0.10	11.5 ^{+1.1} _{-2.1}	C	a,e,w
NGC 1407	28.8	-21.92	0.93	0.083	<4.7	1.67±0.07	4.88±0.06	2.85±0.03	6.6 ^{+1.9} _{-1.5}	G	a,e,x
NGC 2865	37.8	-20.84	0.78	0.193	5.3	3.19±0.05	3.06±0.04	2.69±0.03	1.1 ^{+0.0} _{-0.0}	F	a,k,z
NGC 2974	21.5	-20.05	0.95	0.110	5.8	1.95±0.10	4.77±0.11	2.78±0.10	3.0 ^{+1.0} _{-0.6}	F	a,l,v
NGC 2986	30.7	-21.03	0.99	0.045	<5.3	1.48±0.06	4.97±0.05	2.92±0.03	11.0 ^{+1.6} _{-1.2}	F	b,e,x
NGC 3078	35.2	-21.01	0.97	0.103	<7.0	1.12±0.09	5.20±0.07	3.16±0.04	12.6 ^{+0.0} _{-0.3}	F	a,e,x
NGC 3258	32.1	-20.42	0.92	0.123	<5.8	1.57±0.09	5.08±0.09	3.11±0.09	6.9 ^{+2.6} _{-2.1}	G	a,e,v
NGC 3268	34.8	-20.87	0.96	0.087	<6.9	1.01±0.11	4.97±0.11	2.64±0.10	12.6 ^{+0.0} _{-0.3}	C	a,e,v
NGC 3557	45.7	-22.38	0.87	0.111	<11.8	1.75±0.08	4.72±0.08	3.00±0.08	4.7 ^{+1.6} _{-1.1}	G	a,e,v
NGC 3557B	38.2	-19.82	0.86	0.182	<8.3	-	-	-	-	G	c,e
NGC 3585	20.0	-20.98	0.91	0.048	<2.3	-	-	-	-	F	a,e
NGC 3640	27.0	-21.03	0.92	0.142	<0.2	1.96±0.06	4.57±0.08	3.09±0.09	2.6 ^{+0.3} _{-0.2}	F	a,i,y
NGC 3706	37.4	-20.96	0.93	0.120	<7.9	-	-	-	-	U	c,e
NGC 3904	28.3	-20.80	0.94	0.108	12.7	-	-	-	-	U	a,m
NGC 3923	22.9	-21.41	0.95	0.100	<3.0	1.87±0.08	5.12±0.07	3.07±0.04	2.8 ^{+0.3} _{-0.1}	U	a,e,x
NGC 3962	35.3	-21.35	0.95	0.059	27.9	2.02±0.08	4.79±0.07	2.81±0.07	2.5 ^{+0.4} _{-0.3}	F	a,n,v
NGC 4105	26.5	-20.85	0.87	0.109	7.8	-	-	-	-	F	a,o
NGC 4261	31.6	-21.26	0.98	0.053	<5.7	1.34±0.06	5.11±0.04	3.01±0.04	12.6 ^{+0.0} _{-0.6}	C	a,e,x
NGC 4365	20.4	-21.16	0.97	0.070	<0.4	-	-	-	-	C	a,i
NGC 4472	16.3	-21.90	0.97	0.000	0.5	1.62±0.06	4.85±0.06	2.91±0.05	7.6 ^{+1.7} _{-1.0}	C	a,p,x
NGC 4636	14.7	-20.54	0.93	0.066	8.1	1.58±0.13	5.07±0.12	2.96±0.16	7.6 ^{+3.0} _{-3.0}	F	a,q,v
NGC 4645	29.9	-20.12	0.95	0.000	<5.1	-	-	-	-	C	a,e
NGC 4696	35.5	-21.62	0.94	0.075	<7.1	1.75±0.19	4.52±0.25	2.34±0.26	8.1 ^{+4.2} _{-3.7}	C	a,e,v
NGC 4697	11.7	-20.24	0.92	0.091	<0.6	1.75±0.07	4.08±0.05	2.77±0.04	7.2 ^{+1.7} _{-1.5}	C	a,i,x
NGC 4767	32.8	-20.57	0.93	0.000	<6.1	-	-	-	-	C	a,e
NGC 5011	41.9	-21.20	0.89	0.077	<9.9	1.78±0.13	4.61±0.15	2.70±0.15	5.6 ^{+3.1} _{-1.9}	U	a,e,v
NGC 5018	40.5	-21.80	0.85	0.184	7.4	2.39±0.06	3.51±0.09	2.85±0.10	1.8 ^{+0.1} _{-0.1}	F	c,r,y
NGC 5044	31.2	-21.23	0.98	0.041	<5.5	2.44±0.28	4.58±0.25	2.56±0.24	1.7 ^{+0.5} _{-0.2}	G	a,e,v
NGC 5061	29.1	-21.44	0.85	0.104	<4.8	-	-	-	-	F	a,e
NGC 5077	38.0	-20.82	0.98	0.061	15.4	1.66±0.12	4.92±0.11	2.98±0.11	5.9 ^{+3.4} _{-2.1}	G	c,d,v
NGC 5576	25.5	-20.40	0.88	0.122	<0.4	-	-	-	-	F	a,s
NGC 5638	26.3	-20.11	0.94	0.036	<0.3	1.65±0.04	4.64±0.04	2.84±0.04	8.1 ^{+0.8} _{-1.2}	F	a,t,x
NGC 5812	26.9	-20.36	0.94	0.080	<4.1	1.70±0.04	4.81±0.04	3.06±0.04	5.0 ^{+0.9} _{-0.6}	F	a,e,x
NGC 5813	32.2	-21.30	0.95	0.054	<1.0	1.42±0.07	4.65±0.05	2.67±0.05	12.6 ^{+0.0} _{-0.6}	G	a,i,x
NGC 5846	24.9	-21.16	0.98	0.068	3.5	1.45±0.07	4.93±0.05	2.86±0.04	12.0 ^{+0.6} _{-0.6}	G	a,o,x
NGC 5898	29.1	-20.54	0.92	0.114	<4.8	1.78±0.17	4.30±0.17	2.56±0.15	6.8 ^{+1.6} _{-2.6}	G	a,u,v
NGC 5903	33.9	-21.13	0.89	0.075	9.2	1.68±0.10	4.44±0.08	2.90±0.05	7.4 ^{+2.6} _{-2.0}	G	a,u,x
NGC 6861	28.1	-20.44	0.95	0.123	<4.5	-	-	-	-	G	a,e
NGC 6868	26.8	-20.75	0.97	0.096	<4.1	1.84±0.10	5.05±0.10	3.04±0.09	2.9 ^{+0.9} _{-0.3}	G	a,e,v
NGC 6958	33.1	-20.53	0.86	0.122	<6.2	1.63±0.05	3.89±0.04	2.75±0.03	10.7 ^{+1.0} _{-0.7}	C	c,e,x
NGC 7029	38.4	-20.72	0.86	0.085	<8.4	-	-	-	-	G	a,e
NGC 7144	24.5	-20.38	0.91	0.100	<3.4	-	-	-	-	G	a,e
NGC 7192	37.8	-20.85	0.92	0.096	<8.1	1.71±0.12	4.66±0.11	3.17±0.10	4.8 ^{+3.0} _{-1.6}	F	a,e,v
NGC 7196	45.1	-21.03	0.91	0.171	<11.5	-	-	-	-	G	a,e
NGC 7507	25.0	-20.85	0.94	0.084	<3.5	-	-	-	-	F	a,e

(1) Distance from: (a) Tonry et al. (2001); (b) NED recession velocity corrected for Virgo infall ($h = 0.73$); (c) NED z -independent. (2) M_B derived from HyperLeda *btc*. (3) Colour as in T09. (4) T_c from T09. (5) $M(\text{H I})$ adopting the total H I flux from: (d) Oosterloo (priv. comm.); (e) HIPASS spectra (Meyer et al. 2004); (f) Oosterloo et al. (2007); (g) Haynes et al. (1990); (h) Sansom et al. (2000); (i) Knapp et al. (1985); (j) Huchtmeier (1994); (k) Schiminovich et al. (1995); (l) Weijmans et al. (2008); (m) Bottinelli & Gouguenheim (1977); (n) Bottinelli & Gouguenheim (1979b); (o) Bottinelli & Gouguenheim (1979a); (p) McNamara et al. (1994); (q) Knapp et al. (1978); (r) Kim et al. (1988); (s) Lake & Schommer (1984); (t) Lewis (1987); (u) Appleton et al. (1990); see text for the calculation of the upper limits. (6-8) Line-strength indices from: (v) Annibali et al. (2006); (w) Trager (priv. comm.); (x) Thomas et al. (2005); (y) Serra et al. (2008); (z) Sánchez-Blázquez et al. (2007); $\langle\text{Fe}\rangle = (\text{Fe}5270 + \text{Fe}5335)/2$. (9) t_{SSP} derived in this work. (10) Environment from T09.